$LiSrAlF_6$ with the $LiBaCrF_6$-type structure

2004 J. Phys.: Condens. Matter 16 3005

(http://iopscience.iop.org/0953-8984/16/18/001)

INSTITUTE OF PHYSICS PUBLISHING JOURNAL OF PHYSICS: CONDENSED MATTER

J. Phys.: Condens. Matter **16** (2004) 3005–3013 PII: S0953-8984(04)76381-X

$LiSrAlF_6$ with the $LiBaCrF_6$-type structure

Andrzej Grzechnik[1,5], Vladimir Dmitriev[2], Hans-Peter Weber[2,3], Jean-Yves Gesland[4] and Sander van Smaalen[1]

[1] Laboratory of Crystallography, University of Bayreuth, D-95440 Bayreuth, Germany
[2] Group 'Structure of Materials under Extreme Conditions', Swiss-Norwegian Beamlines, European Synchrotron Radiation Facility, BP 220, F-38043 Grenoble cedex, France
[3] Laboratoire de Cristallographie, EPFL/SB/IPMC/LCR, École Polytechnique Fédéral de Lausanne, CH-1015 Lausanne, Switzerland
[4] Université du Maine-Cristallogenese, F-72025 Le Mans cedex, France

E-mail: andrzej@uni-bayreuth.de

Received 16 February 2004
Published 23 April 2004
Online at stacks.iop.org/JPhysCM/16/3005
DOI: 10.1088/0953-8984/16/18/001

Abstract

The crystal structure of $LiSrAlF_6$-III ($P2_1/c$, $Z = 4$) occurring above 3.0 GPa at room temperature was studied with synchrotron angle-dispersive x-ray powder diffraction in a diamond anvil cell. It was solved by combining a global optimization and a topological analysis with the Rietveld method using rigid-body AlF_6 geometrical constraints. $LiSrAlF_6$-III, related to $LiBaCrF_6$ ($P2_1/c$, $Z = 4$), is built of deformed SrF_{12} icosahedra within a three-dimensional framework of corner-sharing distorted AlF_6 octahedra and LiF_4 tetrahedra, whereas the low-pressure phases I ($P\bar{3}1c$, $Z = 2$) and II ($P2_1/c$, $Z = 4$) have cations exclusively in distorted octahedral coordinations. The pressure-induced changes of the coordination polyhedra in the series $LiSrAlF_6$-I, $LiSrAlF_6$-II to $LiSrAlF_6$-III are similar to the differences in coordination polyhedra due to the increase of the ionic radii of the Sr^{2+} and Ba^{2+} cations in $LiSrAlF_6$-I and $LiBaM''F_6$ (M'' = Al, Ga, Cr, V, Fe, or Ti) at ambient conditions. These observations are discussed on the basis of the high-pressure high-temperature systematics in AB_2X_6 compounds.

(Some figures in this article are in colour only in the electronic version)

1. Introduction

The crystal structures and topologies of $MM'M''F_6$ fluorides at ambient conditions are usually interpreted as close packings of F^{1-} anions with the cations occupying available voids [1]. The actual structure type is governed by the relative sizes of the cations. If a fluoride comprises large

[5] Author to whom any correspondence should be addressed.

cations, an alternative description has been given in terms of packings of the $M''F_6^{3-}$ complex ions with the M and M′ atoms in the voids. The colquiriite family of fluoride compounds $LiM'M''F_6$ (M′ = Ca or Sr; M″ = Al, Ga, or Cr), with each cation at a deformed octahedral site within the hcp arrangement of fluorines ($P\bar{3}1c$, $Z = 2$), belongs to this group [2]. $LiSrAlF_6$ is an ordered derivative of the Li_2ZrF_6 structure type ($P\bar{3}1m$, $Z = 1$). The stability and distortions of the colquiriite structure at atmospheric conditions have been previously discussed on the basis of ionic radii [2, 3]. The compounds $LiBaM''F_6$ (M″ = Al, Ga, Cr, V, Fe, or Ti; $P2_1/c$, $Z = 4$) do not possess this structure [4]. Instead, Ba atoms are in icosahedral coordination by F atoms within a framework of corner-linked LiF_4 tetrahedra and $M''F_6$ octahedra [4]. On the other hand, when the M′ atoms are Mg, Mn, Co, Ni or Zn, the $LiM'M''F_6$ fluorides have the trirutile ($P4_2/mnm$, $Z = 2$) or Na_2SiF_6 ($P321$, $Z = 3$) type structures, with all the cations octahedrally coordinated to fluorines.

Our interest in $LiSrAlF_6$ ($P\bar{3}1c$, $Z = 2$) arises from the fact that it is considered to be the most promising class of materials for optical applications like laser hosts and scintillating materials [2, 3, 5]. Recently, we have reported the high-pressure structure $LiSrAlF_6$-II ($P2_1/c$, $Z = 4$) that is a distorted variant of the ambient pressure polymorph ($LiSrAlF_6$-I) stable between 1.6 and 3.0 GPa [6]. $LiCaAlF_6$ transforms to an isostructural polymorph II above about 7 GPa. The understanding of pressure-induced phase transitions, structures and optical properties of the colquiriite materials could be improved by further investigations of the transformations involving changes in coordination spheres of the cations. Phonon energies, influencing luminescence efficiencies [5], are structure dependent and could be lowered by pressure-induced phase transitions to the polymorphs with increased coordination numbers around luminescent sites. In this paper, we report on the crystal structure of $LiSrAlF_6$ above 3.0 GPa studied *in situ* in a diamond anvil cell with synchrotron angle-dispersive x-ray powder diffraction. We also discuss the high-pressure high-temperature systematics of the AB_2X_6 compounds.

2. Experimental details

A single crystal of $LiSrAlF_6$, grown by the Czochralski method, was ground into a fine powder in ethanol and loaded into a diamond anvil cell with argon as a pressure transmitting medium. Angle-dispersive powder x-ray diffraction patterns were measured at room temperature on the Swiss-Norwegian Beamlines at the European Synchrotron Radiation Facility (BM1A, ESRF, Grenoble, France). Monochromatic radiation at 0.719 98 Å was used for data collection on an image plate (MAR345). The images were integrated using the program FIT2D [7] to yield diagrams of intensity versus 2θ. The ruby luminescence method [8] was used for pressure measurements.

3. Results and discussion

Diffraction patterns of $LiSrAlF_6$ at different pressures are shown in figures 1 and 2. Between 1.6 and 3.0 GPa upon compression at room temperature, the stable structure is $LiSrAlF_6$-II ($P2_1/c$, $Z = 4$) [6]. Above 3.0 GPa (figure 1), there occurs a phase transition to another modification of $LiSrAlF_6$, here called $LiSrAlF_6$-III (figure 1). The lower (II) and higher (III) pressure phases coexist at least up to 5.7 GPa.

Structure solution of $LiSrAlF_6$-III would have been hampered by the presence of diffraction from both phases II and III in each measured diagram above 3 GPa. A single-phase sample of $LiSrAlF_6$-III was thus obtained by annealing at 5.7 GPa and 423 K for 3 h. Subsequently,

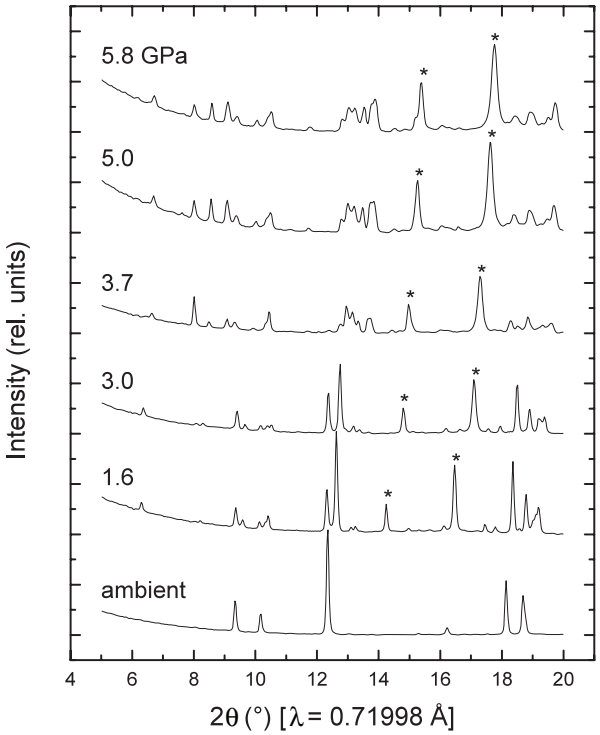

Figure 1. Selected powder patterns of $LiSrAlF_6$ upon compression with argon as a pressure medium. Reflections due to argon are marked with stars.

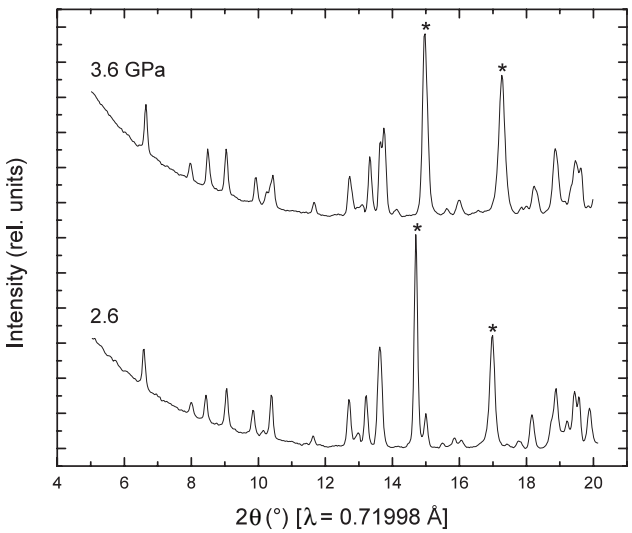

Figure 2. Selected powder patterns of $LiSrAlF_6$ upon decompression after annealing at 423 K for 3 h with argon as a pressure medium. Reflections due to argon are marked with stars.

the sample was allowed to cool down to room temperature and the pressure was lowered to about 3.0 GPa. Diffraction patterns were recorded at 3.6 and 2.6 GPa. They were found to be

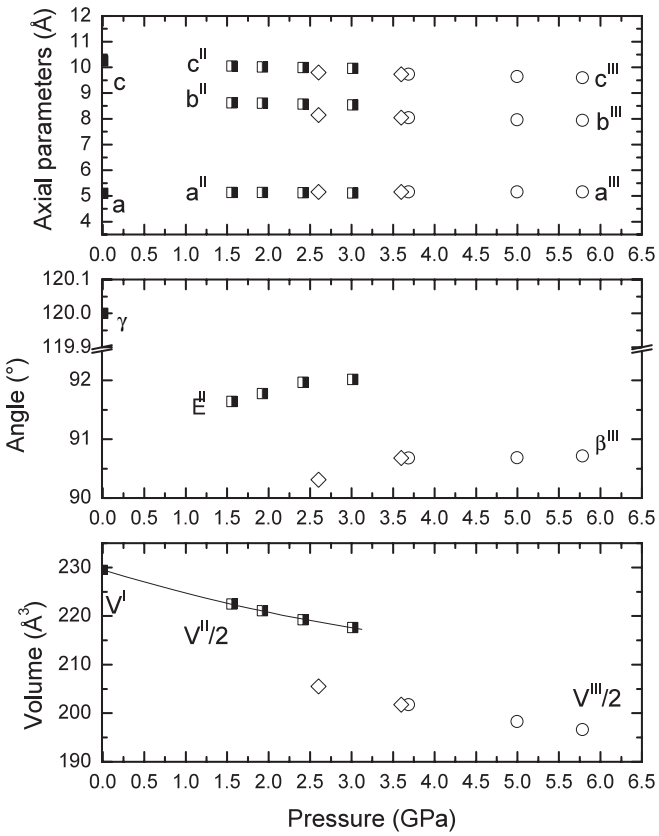

Figure 3. Pressure dependence of lattice parameters and unit cell volumes in $LiSrAlF_6$ up to 6.0 GPa. Full, half open and open symbols stand for the $LiSrAlF_6$-I, $LiSrAlF_6$-II and $LiSrAlF_6$-III polymorphs, respectively. Open circles and diamonds stand for the data upon compression and decompression, respectively. For clarity, the unit cell volumes of the monoclinic phases are divided by a factor of two. The curve represents the equation-of-state fit to the unit cell volumes of $LiSrAlF_6$-I and $LiSrAlF_6$-II [6].

entirely due to the phase III (figure 2). At still lower pressures, $LiSrAlF_6$-III transforms back to $LiSrAlF_6$-II. The pattern collected at 2.6 GPa after annealing upon decompression was used for indexing. The first 20 reflections were indexed using the program DICVOL91 [9] with a monoclinic unit cell: $a = 5.1542(6)$ Å, $b = 9.795(1)$ Å, $c = 8.126(1)$ Å, $\beta = 90.29(1)°$, $V = 410.3(2)$ Å^3, $M(20) = 14.0$, $F(20) = 42.9(0.0097, 48)$. The systematic absences indicated that the space group is $P2_1/c$ [10].

The pressure dependence of the lattice parameters in $LiSrAlF_6$-I ($P\bar{3}1c$, $Z = 2$), $LiSrAlF_6$-II ($P2_1/c$, $Z = 4$) and $LiSrAlF_6$-III ($P2_1/c$, $Z = 4$) is plotted up to about 6 GPa in figure 3. The compression data for both $LiSrAlF_6$-I and $LiSrAlF_6$-II to 3 GPa could be fitted by a common Birch equation of state [6, 11], resulting in the zero-pressure bulk modulus $B_0 = 49(1)$ GPa ($B' = 4.0$ and $V_0 = 229.51$ Å^3). However, there is a discontinuity in the pressure evolution of the unit cell volumes at the phase transition II → III with a relative volume change of 6% at 3.0 GPa. This result shows that the phase transformation II → III is of first order and that major structural rearrangements can be expected, despite the fact that $LiSrAlF_6$-II and $LiSrAlF_6$-III have the same space group and the same number of formula units in the unit cell ($P2_1/c$, $Z = 4$).

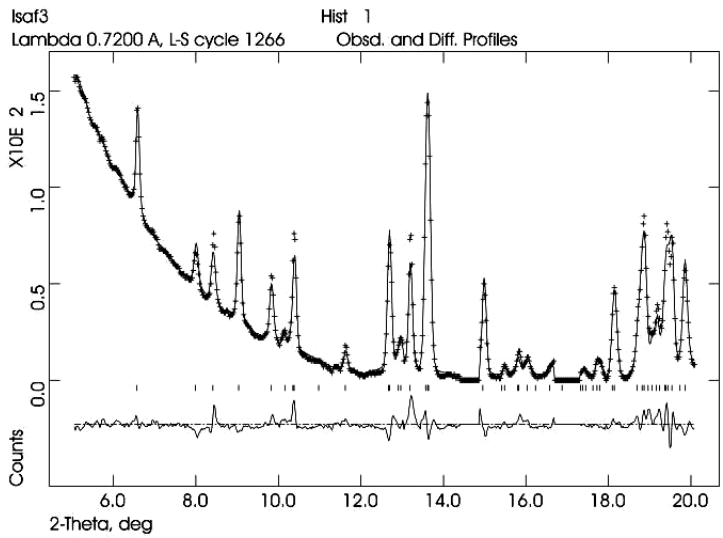

Figure 4. Observed, calculated and difference x-ray powder patterns for $LiSrAlF_6$-III ($P2_1/c$, $Z = 4$) at 2.6 GPa as obtained after the final Rietveld refinement. Vertical markers indicate the positions of Bragg reflections. The 2θ regions 14.40°–14.88° and 16.70°–17.30°, in which two reflections due to argon are observed, were excluded from the Rietveld refinement.

The crystal structure of $LiSrAlF_6$-III was partially solved with the global optimization algorithm FOX [12] against the pattern collected at 2.6 GPa upon decompression (figures 2 and 4). Since the ratio of the number of observed Bragg peaks to the number of structural parameters was expected to be very low (50 reflections, all atoms in the general positions 4e), the number of optimized parameters was drastically reduced by introducing an octahedron around the Al atoms with Al–F bond distances initially equal to 1.8 Å, i.e. equal to the average distances in the ambient pressure structure $LiSrAlF_6$-I ($P\bar{3}1c$, $Z = 2$) [2] and in pressure-induced $LiSrAlF_6$-II ($P2_1/c$, $Z = 4$) [6]. Bonding and angular distortions of the AF_6 octahedra, i.e. the AlF_6^{3-} complex anion [1], were accounted for by relaxing delta and sigma parameters in the program FOX [12]. The solution was reached in about 150 000 trial configurations. However, the Li atoms could not be properly located using this method and some of the Li–F distances were anomalously short. Thus, the entire procedure was carried out without the Li atoms to obtain the $SrAlF_6^{1-}$ sublattice.

The topological analysis of the globally optimized $SrAlF_6^{1-}$ sublattice with all the atoms at the general positions 4e was carried out using the program DIRICHLET of the TOPOS package [13]. Voronoi–Dirichlet polyhedra (VDP) for the first coordination spheres of the fluorine sublattice were constructed to determine its geometric and topological characteristics. Each of the six non-equivalent fluorine atoms was chosen in turn to be at the origin of the sublattice in the search for the VDP vertices that represent the voids in the crystal structure, i.e. in the anionic F^{1-} sublattice. The globally optimized coordinates of the Sr and Al atoms were easily identified as some of the VDP vertices. The coordinates of the remaining VDP vertices and their connectivities, i.e. distances between the voids and the Sr^{2+}, Al^{3+} and F^{1-} ions, respectively, were further scrutinized to obtain atomic coordinates for the lithium atoms. This procedure was based on the principle that cations tend to be arranged as uniformly as possible in the space available [1]. The only voids for which the hypothetical Li–Li, Li–Sr and Li–Al distances in the cationic sublattice as well as the hypothetical Li–F bond lengths

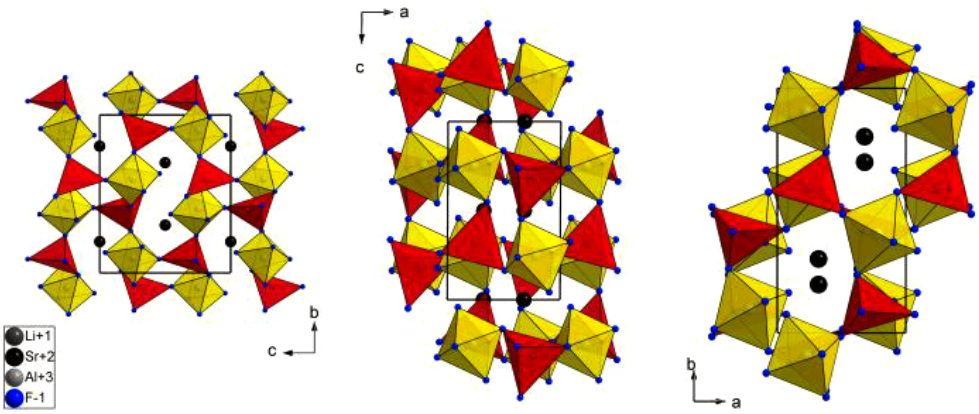

Figure 5. Projections of the crystal structure of $LiSrAlF_6$-III ($P2_1/c$, $Z = 4$).

were crystallographically acceptable [1, 13], turned out to be the ones with the tetrahedral coordination to the F atoms. The voids with the octahedral coordination possessed too short distances to the Sr^{2+} and Al^{3+} cations.

The complete $LiSrAlF_6$-III structural model, i.e. the globally optimized $SrAlF_6^{1-}$ substructure and the Li^{1+} cations from the crystal topology considerations, was subsequently used for the structure refinement against the observed pattern at 2.6 GPa with the Rietveld method using the program GSAS [14] (figure 4). The best fit was obtained at $R_{wp} = 19.67\%$, $R_p = 9.94\%$, and $R(F^2) = 15.61\%$ (the residuals R_{wp} and R_p have been calculated with the background eliminated, see the GSAS manual). To reduce the number of structural variables, a rigid AlF_6 octahedron centred at the Al atom was introduced. The GEOMETRY subroutine was used to determine the orthonormal coordinates and rotation angles $R_1(X)$, $R_2(Y)$, and $R_3(Z)$ for the AlF_6^{-3} complex anion. The refined parameters for the rigid body were: $R_1(X)$, $R_2(Y)$ and $R_3(Z)$ rotation angles, $T(X)$, $T(Y)$ and $T(Z)$ translations, and an isotropic translational tensor ($T_{11} = T_{22} = T_{33}$) in the TLS formalism. The additional variables were: Li and Sr atomic positions, the isotropic thermal parameter for the Sr atom $U_i/U_e * 100 = 1.6(4)$, lattice parameters, scale factor and Stephens profile function [15]. The conventional fractional coordinates for all the atoms and selected interatomic distances are given in table 1.

The crystal structure of $LiSrAlF_6$-III in different projections is shown in figure 5. It consists of corner-sharing distorted AlF_6 octahedra and LiF_4 tetrahedra forming a three-dimensional network. The shortest AlF_6 inter-octahedral F–F distance is 2.44 Å. The Sr atoms are no longer octahedrally coordinated to the fluorine atoms in a distorted hcp array. Instead, the coordination polyhedron around the Sr atoms could be considered as a largely deformed SrF_{12} icosahedron (figure 6). The twelve distances to fluorines in the first coordination sphere of the strontium atoms vary from 2.27 to 3.42 Å, with the average Sr–F distance of 2.75 Å. Three Sr–F bond lengths are larger than 3.0 Å. The Sr–F average for the remaining nine is 2.59 Å. The average Sr–F distance in the SrF_6 octahedra in phases I ($P\bar{3}1c$, $Z = 2$) and II ($P2_1/c$, $Z = 4$) are 2.42 Å [2] and 2.43 Å [6], respectively. The average Li–F bond length of 1.86 Å in the LiF_4 tetrahedra in $LiSrAlF_6$-III is shorter than the Li–F distances in LiF_6 octahedra in the phases I (2.02 Å) [2] and II (2.08 Å) [6].

The pressure-induced structure of $LiSrAlF_6$-III resembles the structure of the $LiBaM''F_6$ compounds (M″ = Al, Ga, Cr, V, Fe, or Ti) at ambient conditions [4]. In this type, BaF_{12} icosahedra are within a framework of corner-linked LiF_4 tetrahedra and $M''F_6$ octahedra

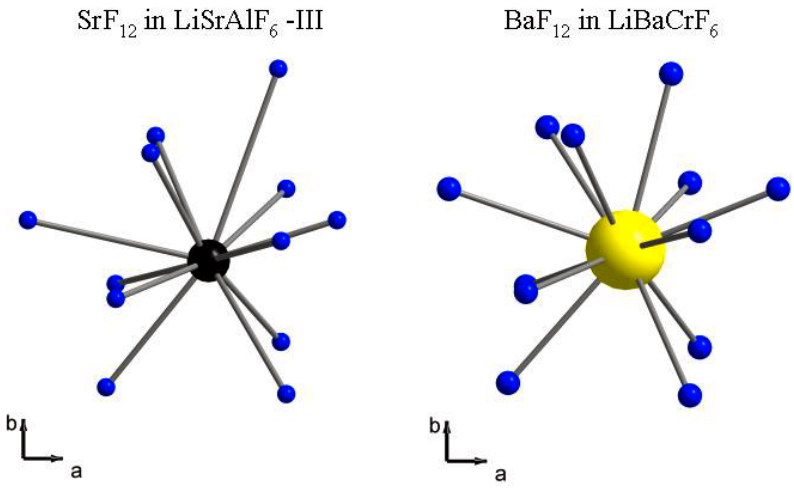

Figure 6. SrF_{12} and BaF_{12} coordinations in $LiSrAlF_6$-III and $LiBaCrF_6$ [4], respectively.

Table 1. Structural parameters for $LiSrAlF_6$-III ($P2_1/$, $Z = 4$) at 2.6 GPa—$a = 5.1539(7)$ Å, $b = 9.798(2)$ Å, $c = 8.139(1)$ Å, $\beta = 90.31(2)°$. Estimated standard deviations are given in parenthesis.

Atom	x	y	z
Li	0.242(26)	0.589(16)	0.181(17)
Sr	0.3206(12)	0.1977(6)	−0.0003(16)
Al	0.2221(27)	0.9051(14)	0.2501(16)
F1	0.069(4)	0.0753(16)	0.2626(31)
F2	0.348(4)	0.9130(25)	0.4512(18)
F3	0.4917(34)	0.9854(20)	0.1633(22)
F4	0.095(4)	0.8712(26)	0.0422(17)
F5	−0.0862(29)	0.8358(21)	0.3229(22)
F6	0.3792(34)	0.7374(16)	0.2378(34)
	Selected distances (Å)		
Li–F1	1.67(14)	Li–F2	2.93(15)
Li–F2	1.96(15)	Li–F3	2.12(12)
Li–F5	2.61(15)	Li–F6	1.68(15)
Sr–F1	2.780(27)	Sr–F1	3.214(22)
Sr–F2	2.741(24)	Sr–F3	2.620(21)
Sr–F3	2.435(20)	Sr–F4	3.422(27)
Sr–F4	2.270(19)	Sr–F4	3.107(20)
Sr–F5	2.322(20)	Sr–F5	2.903(23)
Sr–F6	2.659(29)	Sr–F6	2.563(27)
Al–F1	1.848 43(24)	Al–F2	1.760 48(30)
Al–F3	1.749 42(23)	Al–F4	1.841 06(31)
Al–F5	1.829 46(25)	Al–F6	1.834 65(24)

($P2_1/c$, $Z = 4$). The packing of $M''F_6$ octahedra and LiF_4 tetrahedra in $LiSrAlF_6$-III and $LiBaCrF_6$ are very similar. The BaF_{12} icosahedra in $LiBaM''F_6$ at ambient conditions are less distorted than the SrF_{12} icosahedron in $LiSrAlF_6$-III at high pressures (figure 6). The Ba–F distances in $LiBaCrF_6$ range from 2.6 to 3.17 Å, with only three B–F bond lengths exceeding 3.0 Å. The average Li–F bond length in the LiF_4 tetrahedra is 1.87 Å.

Galy and Anderson [16] proposed simple high-pressure high-temperature transformation mechanisms of the Li_2ZrF_6 type ($P\bar{3}1m$, $Z = 1$) through cation rearrangements in the hcp anion array. They also constructed a tentative pressure–temperature phase diagram for the ternary compounds of general formula AB_2X_6. Accordingly, the Li_2ZrF_6 structure would be a high-pressure variant of the trirutile ($P4_2/mnm$, $Z = 2$) or Na_2SiF_6 ($P321$, $Z = 3$) types. Moreover, the AB_2X_6 materials would be expected to transform to the columbite $FeNb_2O_4$ structure ($Pbcn$, $Z = 4$) that is an ordered analogue of the α-PbO_2 type ($Pbcn$, $Z = 4$). These phase transitions are analogous to the ones for the AX_2 compounds as the rutile-type phases transform to the α-PbO_2 structure at high pressures [17, 18]. In each of these structures, all the cations are octahedrally coordinated to the anions [16–19]. The transformations trirutile $\rightarrow$ Li_2ZrF_6 or Na_2SiF_6 $\rightarrow$ Li_2ZrF_6 would correspond to the substitution of the M′ atoms in the LiM′M″F_6 fluorides at atmospheric conditions. The LiM′M″F_6 compounds (M″ = Al, Ga, V, Cr, Fe) have the trirutile or Na_2SiF_6 structures at atmospheric conditions when the M′ atoms (M′ = Mg, Mn, Co, Ni or Zn) are relatively small, while the colquiriite structure, an ordered variant of the Li_2ZrF_6 type, occurs when the M′ atoms are Ca or Sr (M″ = Al, Ga or Cr) [2, 4].

It has been recently shown that the mechanism of phase transitions in the AB_2X_6 compounds through cation rearrangements in the octahedral voids of the anion hcp array at high pressures and high temperatures as proposed by Galy and Anderson [16] is too limited [20]. Li_2ZrF_6 transforms into a polymorph related to the Li_2TbF_6 type ($P2_1/c$, $Z = 4$) [20, 21], in which the zirconium atoms have a bicapped trigonal prismatic coordination forming edge-sharing chains along the *a* axis. Alternatively, the polyhedron around the Zr atoms can be described as a distorted Archimedean square antiprism. The Li^{1+} cations are in two types of coordination: octahedra and square pyramids. The Li_2ZrF_6 structure of the Li_2TbF_6 type [20] could be compared with the one of γ-Na_2UF_6 ($Immm$, $Z = 2$), derived from the ordered fluorite structure [21]. The cubes around the U atoms correspond to the Archimedean antiprisms in the Li_2TbF_6 type due to displacements of fluorines in the (a, c) planes.

The results of our studies on the high-pressure behaviour of $LiSrAlF_6$ also demonstrate the deficiencies of the previously proposed P–T phase diagram for the AB_2X_6 compounds [16]. The pressure-induced coordination change around the strontium atoms during the phase transitions $LiSrAlF_6$-I $\rightarrow$ $LiSrAlF_6$-II $\rightarrow$ $LiSrAlF_6$-III is associated with the decrease of the coordination number of the lithium atoms from 6 to 4. These transformations correspond to the ones at ambient conditions due to the increase of the ionic radii for the Sr^{2+} and Ba^{2+} cations in the series $LiSrAlF_6$-I and LiBaM″F_6 (M″ = Al, Ga, Cr, V, Fe or Ti) [2, 4]. The structure of $LiSrAlF_6$-III could be quenchable to ambient conditions when the Sr atoms are partially substituted by the Ba atoms in the solid solution series $LiSr_{1-x}Ba_xAlF_6$. The pressure-induced coordination changes in pure $LiSrAlF_6$ as well as the high-pressure synthesis of the Li(Sr, Ba)AlF_6 compounds should thus yield materials with higher cross sections for dopant optical emissions [2].

Acknowledgment

Experimental assistance from the staff of the Swiss-Norwegian Beamlines at ESRF is gratefully acknowledged.

References

[1] Peresypkina E V and Blatov V A 2003 *Acta Crystallogr.* B **59** 361
[2] Yin Y and Keszler D A 1992 *Chem. Mater.* **4** 645

[3] Ono Y *et al* 2001 *J. Cryst. Growth* **229** 505
Pawlak D A *et al* 2001 *J. Cryst. Growth* **233** 699
Martínez Vázquez R *et al* 2002 *J. Cryst. Growth* **237–239** 894
[4] Babel D 1974 *Z. Anorg. Allg. Chem.* **406** 23
Viebahn W and Babel D 1974 *Z. Anorg. Allg. Chem.* **406** 38
[5] Burkhalter R, Dohnke I and Hulliger J 2001 *Prog. Cryst. Growth Charact.* **42** 1
[6] Grzechnik A, Dmitriev V, Weber H-P, Gesland J-Y and van Smaalen S 2004 *J. Phys.: Condens. Matter* **16** 1033
[7] Hammersley A P, Svensson S O, Hanfland M, Fitch A N and Häusermann D 1996 *High Pressure Res.* **14** 235
[8] Piermarini G J, Block S, Barnett J D and Forman R A 1975 *J. Appl. Phys.* **46** 2774
Mao H K, Xu J and Bell P M 1986 *J. Geophys. Res.* **91** 4673
[9] Boultif A and Louer D 1991 *J. Appl. Crystallogr.* **24** 987
[10] Laugier J and Bochu B, CHEKCELL http://www.inpg.fr/LMGP
[11] Birch F 1978 *J. Geophys. Res.* **83** 1257
[12] Favre-Nicolin V and Cerny R 2002 *J. Appl. Crystallogr.* **35** 734
[13] Blatov V A and Shevchenko A P 2003 *Acta Crystallogr.* A **59** 34
[14] Larson A C and von Dreele R B 2000 *GSAS: General Structure Analysis System* Los Alamos National Laboratory
[15] Stephens P W 1999 *J. Appl. Crystallogr.* **32** 281
[16] Galy J and Andersson S 1971 *J. Solid State Chem.* **3** 525
[17] Hyde B G and Andersson S 1989 *Inorganic Crystal Structures* (New York: Wiley)
[18] Leger J M and Haines J 1997 *Eur. J. Solid State Inorg. Chem.* **34** 785
[19] Müller U 1998 *Z. Anorg. Allg. Chem.* **624** 529
[20] Grzechnik A and Gesland J-Y 2003 *Z. Kristallogr. NCS* **218** 3
[21] Laligant Y, Le Bail A, Ferey G, Avignant D and Cousseins J C 1988 *Eur. J. Solid State Inorg. Chem.* **25** 551
Guillot M, El-Ghozzi M, Avignant D and Ferey G 1992 *J. Solid State Chem.* **97** 400